the available diffraction data alone. Second, the agreement between the theoretical and the favored experimental geometry is excellent. The difference is less than one standard deviation for all parameters.

Comparison of the calculated and experimental r_α° geometry of the solid state reveals an rms deviation of 0.015 Å in the bond lengths with a maximum discrepancy of 0.025 Å at CN and an rms deviation of 1.0° in the valence angles with a maximum discrepancy of 1.8° at CCN. The agreement is very satisfactory, particularly if one keeps in mind that the uncertainties in the employed K and δ values are on the order of 0.01 Å. But even more gratifying than the direct comparison is the agreement in many trends of the geometry when the molecule goes from the gaseous to the solid state. First, the experimental increase of the C=O bond length as well as the experimental decrease of the C-N length are matched in direction and magnitude by the calculations. The difference Δ = gas phase value − solid phase value amounts to Δ(exptl) = −0.030 Å for the C=O, to be compared to Δ(calc) = −0.022 Å. For the C-N bond the corresponding values are Δ(exptl) = +0.043 Å and Δ(calc) = +0.021 Å. One may predict that N-H bonds, which take part in hydrogen bonding, will be longer in the solid state than in the gas, whereas C-H bonds, not engaged in hydrogen bonding, are foreseen to be relatively stable. Indeed, these expectations are met in the experimental as well as in the calculated geometry. Second, the valence angles for which the comparison can be made all show the correct trend: for CCO, Δ(exptl) = +1.9° vs Δ(calc) = +0.8°; for CCN Δ(exptl) = −1.4° vs Δ(calc) = −0.5°; for NCO, Δ(exptl) = −0.3° vs Δ(calc) = −0.2°. Third, the experimentally observed rotation of the methyl group is paralleled in our calculations. The difference between the experimental and calculated torsion angle H(3)—C(1)—C(2)=O is only 6.6°. This result strongly indicates that the rotation is indeed a consequence of electrostatic lattice forces, as discussed by Caillet, Claveric, and Pullman.[22] Interestingly, short intermolecular interactions are absent; all contact distances to the methyl group are larger than or equal to van der Waals distances (e.g., $CH_3\cdots CH_3$, 3.930 Å; $CH_3\cdots O$, 3.596 Å; $CH_3\cdots N$, 3.614 Å). This is consistent with the large rms of oscillation (15°) observed for the methyl group by neutron diffraction. The absence of short intermolecular interactions may have played a role in the successful application of the crystal field approach, which emphasizes electrostatic effects and neglects covalent (short range) interactions with neighboring molecules. The calculations also reproduce some subtle details noted in the experimental geometry: the C-H(3) bond, normal to the molecular plane, is longer than the two other C-H bonds, the valence angle C(2)-C(1)-H(3) is smaller than the other CCH angles, while the angle H(1)-C(1)-H(2) is larger than the HCH angles involving H(3). Although perhaps not statistically significant, but gratifying nevertheless, the experimentally observed pyramidization of the amide group is also reproduced in the calculated model, as follows from the torsion angles H(4)—N—C(2)=O and H(4)—N—C(2)—C(1).

Acknowledgment. C.V.A. acknowledges support as a Research Fellow by the Belgian National Science Foundation, NFWO. This work was partly supported by NATO, Research Grant No. 0409/88. The text presents in part results of the Belgian Program on Interuniversity Attraction Poles initiated by the Belgian State—Prime Minister's Office—Science Policy Programming. The scientific responsibility, however, remains with the authors.

Registry No. Acetamide, 60-35-5.

Supplementary Material Available: Charges on atoms before and after the optimalization of the solid-state model (1 page). Ordering information is given on any current masthead page.

(22) Caillet, J.; Claverie, P.; Pullman, B. *Theor. Chim. Acta* **1978**, *47*, 17-26.

Dissociation Dynamics of Perhaloalkoxy Radicals

Zhuangjie Li and Joseph S. Francisco*

Contribution from the Department of Chemistry, Wayne State University, Detroit, Michigan 48202. *Received December 1, 1988*

Abstract: The dissociation dynamics of $CCl_{3-x}F_xO$ radicals have been studied by using ab initio molecular orbital theory. The ab initio calculations suggest that chlorine atom elimination reactions from $CCl_{3-x}F_xO$ are low activation barrier processes, which dominate over fluorine atom dissociation processes. Calculated dissociation rate constants for both Cl and F elimination reactions predict a lifetime that is less than 10^{-10} s for the $CCl_{3-x}F_xO$ radicals. Replacement of two chlorine atoms by two fluorine atoms is found to stabilize the $CCl_{3-x}F_xO$ radicals. The atmospheric implication of these calculations is discussed.

The photochemical dissociation of chlorofluoromethane, CX_3Y (X = Cl or F, and Y = Cl), yields a halogen atom and CX_3 fragment, via

$$CX_3Y + h\nu \rightarrow CX_3 + Y \quad (1)$$

Oxidation of the CX_3 fragment to CX_2O with the release of a halogen atom has been suggested to involve the participation of CX_3O radicals[1-3] via

$$CCl_{3-x}F_x + O \rightarrow CCl_{3-x}F_xO \quad (2)$$

$$CCl_{3-x}F_x + O_3 \rightarrow CCl_{3-x}F_xO + O_2 \quad (3)$$

and

$$CCl_{3-x}F_x + O_2 \rightarrow CCl_{3-x}F_xO_2 \quad (4)$$

$$CCl_{3-x}F_xO_2 + NO \rightarrow CCl_{3-x}F_xO + NO_2 \quad (5)$$

The $CCl_{3-x}F_xO$ species produced as a result of these oxidation steps are atmospherically important since they are responsible for the release of additional halogens from the initial halomethane and engender the production of CX_2O, which have recently been detected in the stratosphere from in situ measurements.[4,5]

(1) Simonaitis, R. In Proceedings of the NATO Advanced Study Institute on Atmospheric Ozone; Report FAA-EE-80-20; Aikin, A, C., Ed.; Washington, D.C., 1980; pp 501-515.

(2) Francisco, J. S.; Williams, I. H. *Int. J. Chem. Kinet.* **1988**, *20*, 455.

(3) Francisco, J. S.; Williams, I. H. In Proceedings of the 16th Annual Meeting of the National Organization of Black Chemists and Chemical Engineers, Chicago, IL, 1989.

0002-7863/89/1511-5660$01.50/0

The kinetics of reactions 4 and 5 have been experimentally studied in detail,[6,7] but evidence of the $CCl_{3-x}F_xO$ was not reported. Indeed, little is known about these radicals. The simplest perhaloalkoxy radical, CF_3O, has only recently been isolated and identified by infrared matrix studies,[8] partly on the basis of our theoretical predictions.[9] The role CF_3O radicals play in possible stratospheric reactions of catalytic importance has been examined previously[10] but not those for other $CCl_{3-x}F_xO$ radicals. Furthermore, the role $CCl_{3-x}F_xO$ radicals play is determined by the competition between the unimolecular dissociations given by

$$CCl_{3-x}F_xO \rightarrow CCl_{2-x}F_xO + Cl \quad (6)$$

$$\rightarrow CCl_{3-x}F_{x-1}O + F \quad (7)$$

$$\rightarrow CCl_{3-x}F_x + O \quad (8)$$

and bimolecular reactions with other atmospherically important species. There have been theoretical decomposition studies of halogenated alkoxy radicals.[11,12] However, those studies employed the semiempirical MNDO method, which did not adequately describe the activation energy barrier for fluorine atom extrusion.[12] Here we report an ab initio calculation of the dissociation of $CCl_{3-x}F_xO$ radicals and supplement our study with RRKM calculations to determine rates of dissociation. We comment on atmospheric implications of the RRKM rates.

Computational Methods

Ab initio molecular orbital calculations were carried out by using the GAUSSIAN 86 program.[13] All equilibrium geometries and transition structures were fully optimized by using an analytical gradient method at both the 3-21G[14] and 6-31G*[15] level. Using Schlegel's method,[16] the geometries were optimized to less than 0.001 Å for distances and 0.1° for angles; both maximum force and rms force were less than 5×10^{-4} au for the optimized structures. To find the transition structure for these reactions, several additional structures along the reaction path were first optimized at the UHF/3-21G level by fixing the C–Cl′ or C–F′ bond and minimizing the energy with respect to all other coordinates. The maximum in the energy profile yielded a suitable initial guess for the Schlegel algorithm. Electron correlations were performed to fourth order[17,18] along with spin projection[19] using Møller–Plesset perturbation theory, including single, double, and quadruple excitation (PMP4SDQ, frozen core). Cartesian force constants were calculated analytically for the reactants and for the transition structures at the UHF/3-21G level. Vibrational frequencies were computed by determining second derivatives of the energy with respect to the Cartesian nuclear coordinates and then transforming them to mass-weighted coordinates.[20]

Results and Discussion

Geometries. Optimized geometries for all reactants and products are listed in Table I. Although the geometries for some of the reactants and products have been published previously, they are reproduced here to facilitate comparison with other structures. Comparisons with the available experimental structures indicate that the overall agreement is very good: ±0.02 Å for bond lengths and ±1.8° for angles at the UHF/6-31G* level.

Geometry optimizations of CF_3O, CF_2ClO, $CFCl_2O$, and CCl_3O radicals suggest the ground state possesses C_s symmetry with the unpaired electron localized mainly on the oxygen atom in the symmetry plane p orbital. Preference for the C_s symmetry may be due to the Jahn–Teller effect, which is well-known to occur in CH_3O[21–23] and CF_3O.[9] The equilibrium geometries of the $^2A'$ and $^2A''$ states on the C_s potential energy surface have been examined. We find that generally the lowest energy equilibrium geometry corresponds to the $^2A'$ state with the exception of CCl_2FO, where the $^2A''$ state is lower than the $^2A'$ state by ca. 5 kcal mol^{-1} at the UMP4/6-31G* level. We note that dissociation of CCl_2FO on the $^2A''$ surface result in electronically excited products that are of higher energy than the ground state. Coupling of the $^2A''$ to the $^2A'$ surfaces through a radiationless path would allow the $^2A''$ state to dissociate CCl_2FO on the $^2A'$ surface. Consequently, all dissociation pathways considered in this study have been examined on the $^2A'$ potential surface.

The minimum energy pathway for chlorine atom elimination in CCl_3O mimics fluorine atom dissociation in CF_3O[10] in that the extrusion process occurs in the symmetrical plane of the molecule containing the oxygen, carbon, and the leaving chlorine atom. The dissociating CCl′ bond in the transition state is predicted to be 2.121 Å (6-31G*) and makes an angle of 93.4° (6-31G*) with the oxygen. For $CClF_2O$ and CCl_2FO, there are two different channels through which the halogen atoms may be eliminated; either through fluorine or through chlorine atom elimination. Chlorine atom elimination from $CClF_2O$ and fluorine atom elimination from CCl_2FO occur, as with CCl_3O, in the symmetry plane of the molecule, thereby retaining the C_s symmetry. However, fluorine atom elimination from CF_2ClO and chlorine atom elimination from CCl_2FO possess no plane of symmetry in the extrusion process, thereby resulting in a reduction of symmetry in the transition state. We note that the loss of the symmetry plane in the dissociation process does not significantly alter geometrical parameters. For example, the predicted dissociating C–Cl′ bond length in $CClF_2O$ (symmetrical transition state) is 2.114 Å (6-31G*) as compared with 2.121Å (6-31G*) for CCl_2FO (unsymmetrical transition state). Similarly, the predicted C–F′ bond length for the extruding fluorine in CCl_2FO is 1.778 Å (6-31G*) as compared with 1.775 Å (6-31G*) for $CClF_2O$. However, the angle made by the oxygen, carbon, and the dissociating halogen atom reveals an interesting trend. For fluorine atom dissociation from $CClF_2O$ and CCl_2FO, no significant change occurs. However, for chlorine atom elimination, the angle widens by 0.7° (6-31G*) in going from $CClF_2O$ to CCl_2FO. This may result as a consequence of the repulsion between two chlorine atoms, which is larger than that between a fluorine atom and a leaving chlorine atom. The undissociating CCl and CF bonds in the transition states of $CClF_2O$ and CCl_2FO are quite similar to the product CClFO. Furthermore, the substitution of one chlorine atom in CCl_2FO by a fluorine atom does not result in significant changes in the geometries, but it does affect the activation energy barrier and enthalpy of dissociation for the extrusion of either chlorine or fluorine.

(4) Rinsland, C. P.; Zonder, R.; Brown, L. R.; Farmer, C. B.; Park, J. H.; Norton, R. H.; Russel III, J. M.; Ruper, O. F. *Geophys. Res. Lett.* **1986**, *11*, 327.
(5) Wilson, S. R.; Crutzen, P. J.; Schuster, G.; Griffith, D. W. T.; Helas, G. *Nature* **1988**, *334*, 689.
(6) Caralp, F.; Lesclaux, R. *Chem. Phys. Lett.* **1983**, *102*, 56.
(7) Ryan, K. R.; Plumb, I. C. *J. Phys. Chem.* **1982**, *86*, 4678.
(8) Andrews, L.; Hawkins, M.; Withnall, R. *Inorg. Chem.* **1985**, *24*, 4234.
(9) Francisco, J. S.; Williams, I. H. *Chem. Phys. Lett.* **1984**, *110*, 240.
(10) Francisco, J. S.; Li, Z.; Williams, I. H. *Chem. Phys. Lett.* **1987**, *140*, 531.
(11) Rayez, J. C.; Rayez, M. T.; Halvick, P.; Duguay, B.; Lesclaux, R.; Dannenberg, J. J. *Chem. Phys.* **1987**, *116*, 203.
(12) Rayez, J. C.; Rayez, M. T.; Halvick, P.; Duguay, B.; Dannenberg, J. J. *Chem. Phys.* **1987**, *118*, 256.
(13) Frisch, M. J.; Binkley, J. S.; DeFrees, D. J.; Raghavachari, K.; Schlegel, H. B.; Whiteside, R. A.; Fox, D. J.; Martin, R. L.; Fleuder, E. M.; Melius, C. F.; Kahn, L. R.; Stewart, J. J. P.; Bobrowicz, F. W.; Pople, J. A. GAUSSIAN 86.
(14) Binkley, J. S.; Pople, J. A.; Hehre, W. J. *J. Am. Chem. Soc.* **1980**, *102*, 939.
(15) Gordon, M. S.; Binkley, J. S.; Pietro, W. J.; Hehre, W. J. *J. Am. Chem. Soc.* **1982**, *104*, 2797.
(16) Schlegel, H. B. *J. Comput. Chem.* **1982**, *3*, 214.
(17) Krishnan, R.; Pople, J. A. *Int. J. Quantum Chem.* **1980**, *14*, 91.
(18) Krishnan, R.; Frish, M. J.; Pople, J. A. *J. Chem. Phys.* **1980**, *72*, 4244.
(19) Schlegel, H. B. *J. Chem. Phys.* **1986**, *84*, 4530.
(20) Schlegel, H. B.; Binkley, J. S.; Pople, J. A. *J. Chem. Phys.* **1984**, *80*, 1976.
(21) Cowell, S. M.; Amos, R. D.; Handy, N. C. *Chem. Phys. Lett.* **1984**, *109*, 525.
(22) Yarkony, D. R.; Schaefer III, H. F.; Rothenburg, S. *J. Am. Chem. Soc.* **1974**, *96*, 656.
(23) Saebo, S.; Radom, L.; Schaefer III, H. F. *J. Chem. Phys.* **1983**, *78*, 845.

Table I. Optimized Geometries for Reactants, Products, and Transition States for $CCl_{3-x}F_xO$ Radial Dissociation[a]

species		basis set 3-21G	basis set 6-31G*	expt	species		basis set 3-21G	basis set 6-31G*	expt
CF_2O	CO	1.169	1.157	1.170[b]		∠FCF	110.0	109.7	
	CF	1.322	1.290	1.316	$[F'\cdots CClFO]^*$	CO	1.248	1.227	
	∠OCF	125.8	125.9	126.2		CCl	1.810	1.720	
CClFO	CO	1.166	1.158	1.173[c]		CF′	1.789	1.775	
	CCl	1.814	1.720	1.725		CF	1.330	1.299	
	CF	1.327	1.300	1.334		∠OCCl	121.1	122.2	
	∠OCCl	125.9	125.7	127.5		∠OCF′	94.1	90.4	
	∠OCF	125.5	124.1	123.7		∠OCF	121.3	120.4	
CCl_2O	CO	1.164	1.159	1.179[d]		∠ClCF′	101.7	104.1	
	CCl	1.830	1.735	1.742		∠ClCF	110.6	111.4	
	∠OCCl	124.9	123.4	124.1		∠F′CF	101.2	100.5	
CF_3	CF	1.329	1.301	1.318[e]	CCl_2FO (X^2A')	CO	1.387	1.359	
	∠FCF	111.6	111.3	111.1[f]		CF	1.344	1.320	
$CClF_2$	CCl	1.832	1.726			CCl	1.844	1.760	
	CF	1.328	1.303			∠OCF	108.0	105.0	
	∠ClCF	112.7	113.6			∠OCCl	110.4	111.0	
	∠FCF	112.0	110.6			∠FCCl	109.4	109.4	
CCl_2F	CF	1.333	1.309			∠ClCCl	109.2	110.8	
	CCl	1.812	1.719		$[F'\cdots CCl_2O]^*$	CO	1.264	1.241	
	∠FCCl	113.2	112.9			CF′	1.772	1.778	
	∠ClCCl	115.2	117.7			CCl	1.820	1.732	
CCl_3	CL	1.793	1.714			∠OCF′	96.1	90.8	
	∠ClCCl	116.3	117.1	116.0[g]		∠OCCl	119.9	119.6	
CF_3O (X^2A')	CO	1.382	1.353			∠F′CCl	101.2	102.6	
	CF′	1.332	1.307			∠ClCCl	112.3	114.1	
	CF	1.332	1.307		$[Cl'\cdots CClFO]^*$	CO	1.291	1.250	
	∠OCF′	107.0	106.8			CF	1.334	1.304	
	∠OCF	111.3	111.3			CCl′	2.128	2.121	
	∠FCF	108.2	107.9			CCl	1.820	1.727	
	∠FCF′	109.5	109.7			∠OCF	118.8	118.5	
$[F'\cdots CF_2O]^*$	CO	1.237	1.218			∠OCCl′	98.1	93.3	
	CF′	1.791	1.762			∠OCCl	117.2	119.8	
	CF	1.322	1.289			∠FCCl′	104.2	102.8	
	∠OCF′	91.7	89.6			∠FCCl	110.1	110.9	
	∠OCF	122.3	122.6			∠Cl′CCl	105.9	107.6	
	∠FCF	109.8	109.8		CCl_3O (X^2A')	CO	1.377	1.350	
	∠FCF′	101.4	101.9			CCl′	1.851	1.768	
$CClF_2O$ (X^2A')	CO	1.369	1.344			CCl	1.839	1.768	
	CCl	1.856	1.755			∠OCCl′	104.5	103.8	
	CF	1.336	1.314			∠OCCl	111.2	110.6	
	∠OCCl	104.4	106.1			∠ClCCl	109.5	119.7	
	∠OCF	112.6	111.2			∠ClCCl′	110.2	111.0	
	∠ClCF	109.2	110.5		$[Cl'\cdots CCl_2O]^*$	CO	1.296	1.263	
	∠FCF	108.6	107.3			CCl′	2.132	2.121	
$[Cl'\cdots CF_2O]^*$	CO	1.290	1.241			CCl	1.827	1.740	
	CCl′	2.136	2.114			∠OCCl′	98.1	93.4	
	CF	1.326	1.292			∠OCCl	117.1	117.5	
	∠OCCl′	96.6	92.6			∠ClCCl	111.6	113.2	
	∠OCF	118.7	120.5			∠ClCCl′	105.1	105.8	
	∠Cl′CF	104.9	104.5						

[a] Bond lengths in angstroms, angles in degrees; refer to Figure 1 for atom labeling. [b] Carpenter, J. H. *J. Mol. Spectrosc.* **1974**, *50*, 182. [c] Oberhammer, H. *J. Chem. Phys.* **1980**, *73*, 4310. [d] Mirri, A. M.; Guarneri, A.; Favero, P.f Zulian, G. *Nuovo Cimento* **1962**, *25*, 265. [e] Yamada, C.; Hirota, E. *J. Chem. Phys.* **1983**, *78*, 1703. [f] Fessenden, R. W.; Schuler, R. H. *J. Chem. Phys.* **1965**, *43*, 2704. [g] Hesse, C.; Leray, N.; Roncin, J. *Mol. Phys.* **1971**, *22*, 137.

Normal Modes. Tables II, III, and IV contain unscaled frequencies and intensities at the UHF/3-21G level for all the reactants, products, and transition states for $CCl_{3-x}F_xO$ dissociation. All the $CCl_{3-x}F_xO$ radicals, in their equilibrium ground state, posses C_s symmetry. Their vibrations span the representation 6a′ + 3a″, and all are infrared and Raman active. Halogen atom dissociation occurring in the symmetry plane also spans the same vibrational representation. Two transition states for CCl_2FO and $CClF_2O$ halogen atom dissociation that take place with C_1 symmetry span the vibrational representation 9a. All vibrations in this representation are also infrared and Raman active. Calculated frequencies of the products from $CCl_{3-x}F_xO$ dissociation compared to experimental ones are overestimated by ~10–15% owing to the use of the harmonic approximation, truncation of the basis set, and neglect of electron correlation in the UHF/3-21G frequency calculation. Nevertheless, calculated frequencies at this level provide correct predictions of the mode ordering. Complemented with estimates of relative intensities, these data provide useful spectroscopic guides to the spectroscopic observations of these species.

Vibrational frequencies for the transition structures are all characterized by one imaginary frequency. One common characteristic of the vibrational frequencies of the transition states is the complex coupling between the modes; this causes some difficulties in defining mode descriptions. In such cases, only the major motions are described. The imaginary frequency for C–Cl′ bond dissociation in CCl_3O, CCl_2FO, and $CClF_2O$ appears to range from 502*i* to 576*i* cm^{-1}. The transition vectors consist mainly of the CCl′ stretching mode. The remaining frequencies of the transition structure, for the most part, lie between the frequencies of the reactants and products. For C–F′ bond extrusion processes, the imaginary frequency for CF_3O, $CClF_2O$, and CCl_2FO transition states are 1059*i*,[10] 877*i*, and 778*i* cm^{-1}, respectively. In this case, the transition vectors for $CClF_2O$ and CCl_2FO show considerable mixing of the CF mode. Interestingly, the substitution of Cl with F, in going from CCl_3O to CF_3O, increases the CO

Table II. Calculated UHF/3-21G Vibrational Frequencies (cm^{-1}) and Intensities (km mol^{-1}) for Reactants, Products, and Transition State for CCl_3O Dissociation

molecule	mode no.	sym	descr	freq		int	
				calcd	exptl	abs	rel
CCl_2O	1	a_1	CO str	2023	1827[a]	364.5	0.64
	2	b_2	CCl str, asym	789	849	574.0	1.00
	3	b_1	CCl_2 wag	586	585	20.14	0.04
	4	a_1	CCl str, sym	505	570	18.66	0.03
	5	b_2	CCl_2 rock	431	440	0.004	0.00
	6	a_1	CCl_2 scissor	285	285	0.990	0.00
CCl_3	1	e	CCl str, asym	858	898[b,c]	154.4	1.00
	2	e	CCl str, asym	858		154.4	1.00
	3	a_1	CCl str, sym	456	460[d]	1.513	0.01
	4	a_1	CCl_3 umbr	314		0.982	0.01
	5	e	CCl_2 twist	256		1.454	0.01
	6	e	CCl_2 wag	256	240[d]	1.454	0.01
CCl_3O (X^2A')	1	a′	CO str	1075		101.3	0.58
	2	a″	CCl_2 rock	808		176.1	1.00
	3	a′	CCl str	747		169.1	0.96
	4	a′	CCl str, sym	489		7.730	0.04
	5	a′	CCl_2 wag	371		4.937	0.03
	6	a′	CCl_3 umbr	331		1.182	0.01
	7	a″	CCl_2 rock	318		3.302	0.02
	8	a′	OCCl′ def/CCl_2 scissor	243		0.051	0.00
	9	a″	CCl_2 twist	196		7.222	0.04
$[Cl'\cdots CCl_2O]^*$	1	a′	CCl′ str	502i		2.982	0.01
	2	a′	CO str	1167		216.9	0.82
	3	a′	CCl str	830		265.6	1.00
	4	a′	CCl str, sym	515		24.70	0.09
	5	a″	CCl_2 rock	388		0.507	0.00
	6	a′	OCCl rock	343		7.565	0.03
	7	a″	CCl_3 umbr	298		1.579	0.01
	8	a′	CCl_2 twist	213		0.144	0.00
	9	a″	OCCl′ def/CCl_2 scissr	183		0.113	0.00

[a] JANAF Themrochemical Tables, 3rd ed.; Chase, Jr., M. W., Davies, C. A., Downey, Jr., J. R., Frurip, D. J., McDonald, R. A., Syverud, A. N. *J. Phys. Chem. Ref. Data, Suppl.* **1985**, *14*. [b] Hesse, C.; Leray, N.; Roncin, J. *Mol. Phys.* **1971**, *22*, 137. [c] Andrews L. *J. Chem. Phys.* **1968**, *48*, 972. [d] Benson, S. W. *J. Chem. Phys.* **1965**, *43*, 2044.

stretching mode for each chlorine replaced.

Energetics

Heats of Reaction. The total energetics for the various equilibrum structures and transition states are listed in Table V. Calculated heats of reaction are provided in Table VI and compared with experimental results; and individual barrier heights are collected in Table VII.

The heats of reaction (Table VI) have been calculated with extended (3-21G) and polarization (6-31G*) basis sets at the Hartree–Fock level with electron correlation. The effect of d orbitals on the heats of reaction is small; but for oxygen atom extrusion, a 6–11 kcal mol^{-1} increase in the energy is predicted. However, electron correlation has a significant effect on the energetics of oxygen atom extrusion; an increase of 41 kcal mol^{-1} is predicted in going from UHF/6-31G* to UMP2/6-31G* level of theory for CCl_3O dissociation to CCl_3 + O. No significant differences are produced in the energetics for the transition states for halogen atom elimination as a consequence of electron correlation and spin projection. For fluorine atom elimination processes, electron correlation and spin projection increases the heat of reaction by 6 kcal mol^{-1}, while heat of reaction for chlorine atom elimination processes decreases, except for CCl_2O + Cl.

Experimental values for the heat of formation for CF_3O[2] and CCl_3O[3] are −156.7 ± 1.5 and −2.8 ± 5 kcal mol^{-1}, respectively. The $\Delta H_f(CF_2O)$ is −152.7 ± 0.4 kcal mol^{-1}, and that for CCl_2O is −52.6 ± 0.8 kcal mol^{-1}. Experimental heats of reactions for

$$CF_3O \rightarrow CF_2O + F \quad (9)$$

$$CCl_3O \rightarrow CCl_2O + Cl \quad (10)$$

are 23.0 ± 1.6 and −20.8 ± 5.1 kcal mol^{-1} at 298 K. Assuming a 0.5 kcal mol^{-1} change of heat of formation for both CF_3O and CCl_3O going from 298 to 0 K, the heats of reaction $\Delta H°$ (0 K) become 23.1 ± 2.0 kcal mol^{-1} for (9) and −20.8 ± 5.6 kcal mol^{-1} for (10). Theoretical heats of reactions are in reasonable agreement with these experimental estimates.

On purely thermodynamic grounds, the energetically most favorable reaction for $CClF_2O$ and CCl_2FO radicals is chlorine extrusion. Fluorine atom extrusion is the next thermodynamically favored reaction; while oxygen atom elimination is the most thermodynamically unfavorable channel of those considered in this study.

There are interesting trends that emerge from these data. The heat of reaction for fluorine atom elimination shows a decreasing trend in going from CF_3O, $CClF_2O$, and CCl_2FO corresponding to 25.2, 21.8, and 13.2 kcal mol^{-1}, respectively. These data suggest that increasing chlorination of CF_3O thermodynamically destabilizes the fluorine atom extrusion process.

Activation Energies. Calculated activation energies for various transition state structures for $CCl_{3-x}F_xO$ dissociation are given in Table VII and are calculated from the total energies given in Table V. Effects of basis sets, higher order electron correlation, and spin projection on the barrier show similar trends to those calculated for the heat of reactions, e.g., changes of ±10 kcal mol^{-1}.

The only experimentally determined activation energy for the $CCl_{3-x}F_xO$ system is trifluoromethoxy radical, CF_3O. Kennedy and Levy[24] measured a value of 31.0 ± 0.5 kcal mol^{-1}. Descamps and Forst[25] measured a value of 26 kcal mol^{-1}, but this value is believed to be too low since a Lindemann extrapolation was used to obtain the rate constant; it is known that this procedure tends to underestimate activation energy. Nevertheless, the present theoretical estimate for the activation energy of 29.1 kcal mol^{-1} is in excellent agreement with that observed by Kennedy and Levy; this also suggests that calculations of the activation energies for $CCl_{3-x}F_xO$ halogen atom extrusion processes are probably underestimated by ca. 2 kcal mol^{-1} at the PMP4/6-31G* level of theory.

With chlorine substitution on CF_3O, there is a large systematic decrease in the activation barrier for fluorine elimination at the

(24) Kennedy, R. C.; Levy, J. B. *J. Phys. Chem.* **1972**, *76*, 3480.
(25) Descamps, B.; Forst, W. *Can. J. Chem.* **1975**, *53*, 1442.

Table III. Calculated UHF/3-21G Vibrational Frequencies (cm^{-1}) and Intensities (km mol^{-1}) for Reactants, Products, and Transition State for CCl_2FO Dissociation

molecule	mode no.	sym	descr	freq calcd	freq exptl	int abs	int rel
CClFO	1	a′	CO str	2086	1868[a]	406.9	0.97
	2	a′	CF str, asym	1238	1095	421.6	1.00
	3	a′	CFO scissor	760	776	150.0	0.36
	4	a″	CFCl wag	690	667	46.32	0.11
	5	a′	CCl str	481	501	2.746	0.01
	6	a′	CFCl scissor	393	415	5.052	0.01
CCl_2O	1	a_1	CO str	2023	1827[a]	364.5	0.64
	2	b_2	CCl str, asym	789	849	574.0	1.00
	3	b_1	CCl_2 wag	586	585	20.14	0.04
	4	a_1	CCl str, sym	505	570	18.66	0.03
	5	b_2	CCl_2 rock	431	440	0.004	0.00
	6	a_1	CCl_2 scissor	285	285	0.990	0.00
CCl_2F	1	a′	CF str	1303	1143[b,c]	217.1	0.71
	2	a″	CCl str, asym	850	919	304.5	1.00
	3	a′	CCl str, sym	574	747	33.78	0.11
	4	a′	CCl_2F umbr	421		5.957	0.02
	5	a″	CFCl rock	355		1.051	0.00
	6	a′	CCl_2 scissor	266		1.312	0.00
CCl_2FO (X^2A')	1	a′	CF str	1289		145.6	0.26
	2	a′	CO str	1113		229.4	0.41
	3	a″	CCl str	864		553.7	1.00
	4	a′	OCF scissor	599		43.70	0.08
	5	a″	CCl_2 rock	437		2.052	0.00
	6	a′	OCF def/CCl_2 scissor	411		0.353	0.00
	7	a′	CCl_2O umbr	400		9.733	0.02
	8	a″	OCF/CCl_2 twist	342		1.016	0.00
	9	a′	CCl_2 wag	261		0.463	0.00
$[F'\cdots CCl_2O]^{\ddagger}$	1	a′	CF str	778*i*		94.83	0.28
	2	a′	CO str	1267		180.9	0.53
	3	a″	CCl str	841		342.6	1.00
	4	a′	CCl str, sym	519		22.06	0.06
	5	a″	CCl_2 rock	400		1.147	0.00
	6	a′	OCF rock	369		5.448	0.02
	7	a′	CCl_2F umbr	302		1.948	0.01
	8	a′	CCl_2 wag	225		0.183	0.00
	9	a″	CCl_2 twist	209		0.040	0.00
$[Cl'\cdots CClFO]^{\ddagger}$	1	a	CCl str	535i		10.41	0.03
	2	a	CF str	1396		302.2	1.00
	3	a	CO str	1113		289.7	0.96
	4	a	FCO rock	697		70.89	0.23
	5	a	CClO/FCO twist	453		3.357	0.01
	6	a	CClF twist	385		10.38	0.03
	7	a	CFO wag	371		4.678	0.02
	8	a	FCO twist	257		0.873	0.00
	9	a	FCCl rock	195		0.228	0.00

[a] JANAF Thermochemical Tables, 3rd ed.; Chase, Jr., M. W., Davies, C. A., Downey, Jr., J. R., Frurip, D. J., McDonald, R. A., Syverud, A. N. *J. Phys. Chem. Refer. Data.* Suppl. **1985**, *14*. [b] Milligan, D. E.; Jacox, M. E.; McAuley, J. H.; Smith, C. E. *J. Mol. Spectrosc.* **1973**, *45*, 377. [c] Prochaska, F. T.; Andrews, L. *J. Chem. Phys.* **1978**, *68*, 5568.

PMP4/6-31G* + ΔZPE level of theory. Substitution of one fluorine in CF_3O by one chlorine decreases the barrier by ca. 1 kcal mol^{-1}; the second reduces the barrier by an additional 6.5 kcal mol^{-1}. Neither basis set effects nor correlation energy corrections are large enough to alter the trend of decreasing activation energy with greater chlorine substitution. Figure 2 (top) emphasizes the trends in the energy profile along the reaction path for fluorine atom dissociation in CF_3O, $CClF_2O$, and CCl_2FO.

An increase in fluorine substitution on CCl_3O appears to increase the activation energy for chlorine atom elimination, except for CCl_2FO, which shows a negative barrier due to an overcorrection by the spin projection method for a small barrier. Nevertheless, the calculation suggests that the addition of chlorine to CClFO (i.e., the reverse of the chlorine atom extrusion process from CCl_2FO) may be barrierless. However, with two fluorine substitutions, the activation energy for chlorine atom extrusion is generally larger than in both CCl_3O and CCl_2FO at all levels of calculations. Figure 2 (bottom) emphasizes the trends in the energy profile along the reaction pathway for chlorine atom extrusion in CCl_3O, CCl_2FO, and $CClF_2O$.

Comparison of activation energies for chlorine and fluorine atom extrusion processes indicate that the former is essentially more favorable than the latter, because of low activation barriers. Thus for reactions that generate CCl_3O, CCl_2FO, and $CClF_2O$ exothermically, the excess energy would be sufficient to drive these radicals to dissociate via reaction 6.

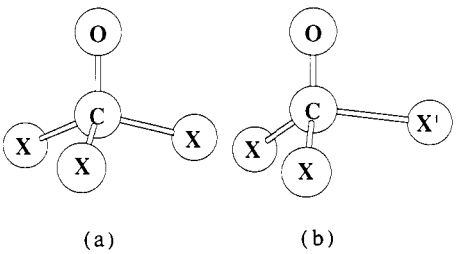

Figure 1. Geometry model of $CCl_{3-x}F_xO$: (a) ground state; (b) transition state.

RRKM Rate Constants

To assess the relative importance of chlorine and fluorine atom substitution on the decomposition kinetics of $CCl_{3-x}F_xO$ radicals, energy-dependent unimolecular dissociation rates are needed. Such rates are obtained from RRKM theory, in which the microca-

Table IV. Calculated UHF/3-21G Vibrational Frequencies (cm^{-1}) and Intensities (km mol^{-1}) for Reactants, Products, and Transition State for $CClF_2O$ Dissociation

molecule	mode no.	sym	descr	freq		int	
				calcd	exptl	abs	rel
CClFO	1	a′	CO str	2086	1868[a]	406.9	0.97
	2	a′	CF str, asym	1238	1095	421.6	1.00
	3	a′	CFO scissor	760	776	150.0	0.36
	4	a″	CFCl wag	690	667	46.32	0.11
	5	a′	CCl str	481	501	2.746	0.01
	6	a′	CFCl scissor	393	415	5.052	0.01
CF_2O	1	a_1	CO str	2132	1928[a]	450.2	1.00
	2	b_2	CF str, asym	1455	1294	407.4	0.90
	3	a_1	CF str, sym	1053	965	35.17	0.08
	4	b_1	CF_2 wag	818	774	83.17	0.18
	5	b_2	CF_2 rock	674	626	24.92	0.06
	6	a_1	CF_2 scissor	598	584	9.646	0.02
CF_2Cl	1	a″	CF str, asym	1421	1208[b,c]	235.6	0.69
	2	a′	CF str, sym	1244	1148	343.3	1.00
	3	a′	CCl str	719	761	148.6	0.43
	4	a″	CF_2 rock	590	599	19.82	0.06
	5	a′	CF_2 wag	384		1.098	0.00
	6	a″	CF_2 twist	341		4.342	0.01
CF_2ClO (X^2A')	1	a″	CF str, asym	1412		276.3	0.90
	2	a′	CO str	1360		305.4	1.00
	3	a′	CF str, sym	1008		195.0	0.64
	4	a′	CF_2O umbr	735		138.1	0.45
	5	a′	CF_2 def	574		16.61	0.05
	6	a″	CF_2 rock	541		12.09	0.04
	7	a′	CCl str/CF_2 wag	426		0.092	0.00
	8	a′	CF_2 wag	329		2.832	0.01
	9	a″	CF_2 twist	183		1.193	0.00
$[Cl'\cdots CF_2O]^*$	1	a′	CCl′ str	576*i*		32.97	0.06
	2	a′	CO str	1459		548.5	1.00
	3	a″	CCl str	1457		298.9	0.54
	4	a′	CCl str, sym	916		16.23	0.03
	5	a″	CCl_2 rock	583		15.03	0.03
	6	a′	OCCl rock	572		14.83	0.03
	7	a′	CF_2 wag	419		6.857	0.01
	8	a′	OCCl def/CF_2 scissor	271		2.122	0.00
	9	a′	CF_2 twist	234		0.640	0.00
$[F'\cdots CClFO]^*$	1	a	CF str	877*i*		197.2	0.56
	2	a	CO str	1493		254.5	0.72
	3	a	CCl str	1177		351.7	1.00
	4	a	CFO scissor	722		90.13	0.26
	5	a	ClCO rock	461		2.261	0.01
	6	a	CFO rock	410		10.25	0.03
	7	a	CF_2Cl umbr	388		4.476	0.01
	8	a	CFO twist	268		1.009	0.00
	9	a	CF_2 twist	212		0.111	0.00

[a] JANAF Thermochemical Tables, 3rd ed.; Chase, Jr., M. W., Davies, C. A., Downey, Jr., I. R., Frurip, D. J.; McDonald, R. A.; Syverud, A. N. *J. Phys. Chem. Refer Data, Suppl.* **1985**, *14*, in box. [b] Milligan, D. E.; Jacox, M. E.; McAuley, J. H.; Smith, C. E. *J. Mol. Spectrosc.* **1973**, *45*, 377. [c] Prochaska, F. T.; Andrews, L. *J. Chem. Phys.* **1978**, *68*, 5577.

Table V. Total Energies (Hartrees) for $CCl_{3-x}F_xO$ Dissociation Reactions

system	reactions	3-21G	6-31G*							
		UHF	UHF	UMP2	UMP3	UMP4	PHF	PMP2	PMP3	PMP4
CF_3O	CF_3O	−408.78660	−411.01325	−411.77437	−411.77922	−411.79395	−411.01599	−411.77589	−411.78007	−411.79480
	$[F'\cdots CF_2O]^*$	−408.72303	−410.94246	−411.71312	−411.71593	−411.73467	−410.96099	−411.72820	−411.72615	−411.74489
	$CF_2O + F$	−408.74929	−410.98027	−411.73685	−411.73764	−411.75418	−410.98234	−411.73603	−411.73699	−411.75232
	$CF_3 + O$	−408.70702	−410.91512	−411.62167	−411.63208	−411.64765	−410.91904	−411.62378	−411.63318	−411.64875
$CClF_2O$	$CClF_2O$	−767.14618	−771.03745	−771.76679	−771.78928	−771.79606	−771.04060	−771.76871	−771.78448	−771.79725
	$[Cl'\cdots CF_2O]^*$	−767.13938	−771.01525	−771.75344	−771.76644	−771.78273	−771.03084	−771.76616	−771.77537	−771.79166
	$[F'\cdots CClFO]^*$	−767.08687	−770.97127	−771.70291	−771.71925	−771.73623	−770.99261	−771.72087	−771.73186	−771.74884
	$CF_2O + Cl$	−767.18083	−771.06327	−771.80024	−771.80746	−771.82260	−771.06567	−771.80134	−771.80789	−771.82304
	$CClFO + F$	−767.11638	−771.01093	−771.73305	−771.74551	−771.75917	−771.01302	−771.73401	−771.74647	−771.76013
	$CClF_2 + O$	−767.07410	−770.94721	−771.61757	−771.64112	−771.65427	−770.95155	−771.63256	−771.64244	−771.65561
CCl_2FO	CCl_2FO	−1125.5075	−1131.0583	−1131.7532	−1131.7813	−1131.7918	−113.0612	−1131.7549	−1131.7823	−1131.7929
	$[F'\cdots CCl_2O]^*$	−1125.4638	−1131.0037	−1131.6956	−1131.7392	−1131.7397	−1131.0275	−1131.7159	−1131.7398	−1131.7546
	$[Cl'\cdots CClFO]^*$	−1125.5081	−1131.0454	−1131.7454	−1131.7713	−1131.7857	−1131.0626	−1131.7597	−1131.7816	−1131.7960
	$CCl_2O + F$	−1125.4930	−1131.0445	−1131.7330	−1131.7569	−1131.7684	−1131.0466	−1131.7339	−1131.7579	−1131.7963
	$CClFO + Cl$	−1125.5479	−1131.0939	−1131.7982	−1131.8169	−1131.8304	−1131.0963	−1131.7993	−1131.8174	−1131.8309
	$CCl_2F + O$	−1125.4517	−1130.9854	−1131.6195	−1131.6558	−1131.6663	−1130.9904	−1131.6224	−1131.6575	−1131.6679
CCl_3O	CCl_3O	−1483.8955	−1491.0944	−1491.7569	−1491.7952	−1491.8042	−1491.07979	−1491.7591	−1491.7967	−1491.8056
	$[Cl'\cdots CCl_2O]^*$	−1483.8891	−1491.0789	−1491.7407	−1491.7787	−1491.7909	−1491.0970	−1491.7559	−1491.7900	−1491.8021
	$CCl_2O + Cl$	−1483.9245	−1491.1275	−1491.7981	−1491.8283	−1491.8396	−1491.1300	−1491.7992	−1491.8287	−1491.8322
	$CCl_3 + O$	−1483.8426	−1491.0321	−1491.6292	−1491.6776	−1491.6856	−1491.0380	−1491.6328	−1491.6797	−1491.6877

Table VI. Heats of Reaction (kcal mol^{-1}) for $CCl_{3-x}F_xO$ Dissociation

	CF_3O		$CClF_2O$			CCl_2FO			CCl_3O	
level of theory	$CF_2O + F$	$CF_3 + O$	$CF_2O + Cl$	$CClFO + F$	$CClF_2 + O$	$CClFO + CL$	$CCl_2O + F$	$CCl_2F + O$	$CCl_2O + Cl$	$CCl_3 + O$
UHF/3-21G	23.4	49.9	−21.7	18.7	45.2	−25.4	9.1	35.0	−18.3	33.2
UHF/6-31G*	20.7	61.6	−16.2	16.6	56.6	−22.3	8.7	45.8	−20.8	39.1
UMP2/6-31G*	23.5	95.8	−21.0	21.2	78.9	−28.2	12.7	85.2	−25.9	80.1
UMP3/6-31G*	26.1	92.3	−11.4	27.5	93.0	−22.3	15.3	78.8	−20.8	73.8
UMP4SDQ/6-31G*	30.0	91.8	−16.7	23.1	89.0	−24.2	14.7	78.8	−22.2	74.4
PHF/6-31G*	21.1	60.8	−15.7	17.3	55.9	−22.0	9.2	44.0	−20.1	37.6
PMP2/6-31G*	25.0	95.4	−20.5	21.8	85.4	−27.9	13.2	83.1	−25.2	79.2
PMP3/6-31G*	27.0	92.2	−14.7	23.9	89.1	−22.0	15.3	78.3	−20.1	73.4
PMP4SDQ/6-31G*	26.7	91.6	−16.2	23.3	88.9	−23.9	14.8	78.4	−16.7	74.0
ΔZPE/3-21G	−1.5	−3.0	0.1	−1.5	−2.9	−0.1	−1.6	−2.8	−0.1	−2.3
PMP4SDQ/6-31G* + ΔZPE/3-21G	25.2	88.6	−16.1	21.8	86.0	−24.0	13.2	75.6	−16.8	71.7
exptl[a]	23.0	103.8							−20.8	81.4

[a] Batt, L.; Walsh, R. *Int. J. Chem. Kinet.* **1982**, *14*, 933. Coomber, J. W.; Whittle, E. *Trans. Faraday Soc.* **1968**, *64*, 2130. Krupenie, P. H. *J. Phys. Chem. Ref. Data* **1972**, *1*, 423. Benson, S. W. *J. Chem. Phys.* **1965**, *43*, 2044. Benson, S. W. *Thermochemical Kinetics*, 2nd ed.; 1976.

Table VII. Activation Energies (kcal mol^{-1}) for $CCl_{3-x}F_xO$ Dissociation

	CF_3O	$CClF_2O$		CCl_2FO		CCl_3O
level of theory	$CF_2O + F$	$CF_2O + Cl$	$CClFO + F$	$CClFO + Cl$	$CCl_2O + F$	$CCl_2O + Cl$
UHF/3-21G	39.9	4.3	37.2	−0.4	27.4	4.0
UHF/6-31G*	44.4	13.9	41.5	8.1	34.3	9.7
UMP2/6-31G*	38.4	8.4	40.0	4.9	36.1	10.2
UMP3/6-31G*	39.7	14.3	43.9	6.3	26.4	10.4
UMP4SDQ/6-31G*	37.2	8.4	37.5	3.9	32.7	8.4
PHF/6-31G*	34.5	6.1	30.1	−0.9	21.2	0.6
PMP2/6-31G*	29.9	1.6	30.0	−3.0	24.5	2.0
PMP3/6-31G*	33.8	5.7	33.0	0.4	26.7	4.2
PMP4SDQ/6-31G*	31.3	3.5	30.4	−2.0	24.0	2.2
ΔZPE/3-21G	−2.2	−1.1	−2.2	−1.2	−2.3	−0.9
PMP4SDQ/6-31G* + ΔZPE/3-21G	29.1	2.4	28.2	−3.2	21.7	1.3
exptl	31.0 ± 0.5[a]					

[a] Kennedy, R. C.; Levy, J. B. *J. Phys. Chem.* **1972**, *76*, 3480.

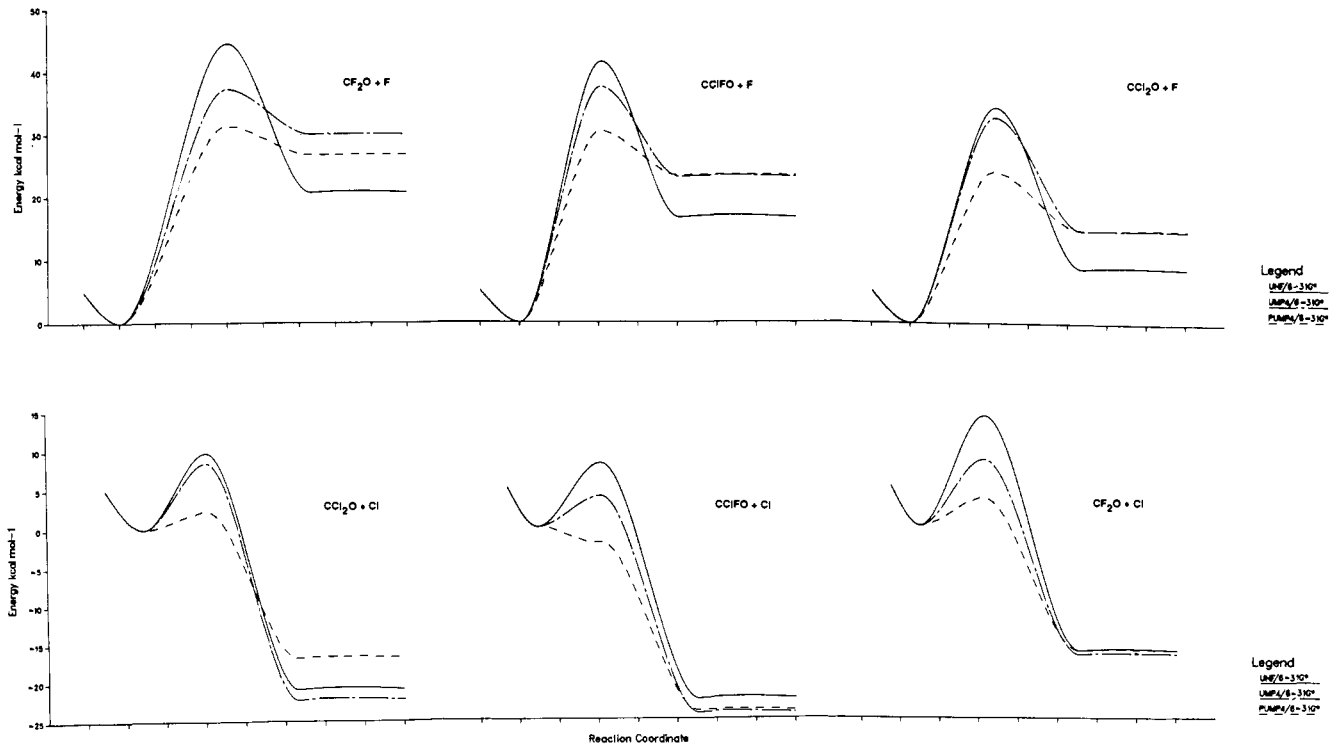

Figure 2. Energy profile for chlorine and fluorine atom elimination processes from $CCl_{3-x}F_xO$ radicals.

nonical unimolecular rate constant, $K(E)$, of an isolated molecule possessing the total energy E is given by

$$K(E) = G(E - E_0)/hN(E) \quad (11)$$

where $G(E-E_0)$ is the sum of states for the transition structure, $N(E)$ is the density of states for the reactant molecule, and h is Plank's constant. Harmonic-state counting by the Hase and Bunker RRKM program[26] was used to compute these quantities.

(26) Hase, W. L.; Bunker, D. L. Program 234, Quantum Chemistry, Program Exchange, Indiana University, Bloomington, 1973.

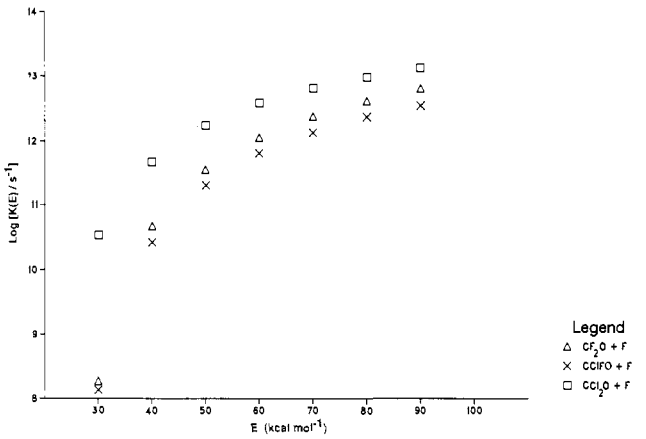

Figure 3. Energy-dependent RRKM rate constants for fluorine atom elimination from CF_3O, $CClF_2O$, and CCl_2FO radicals.

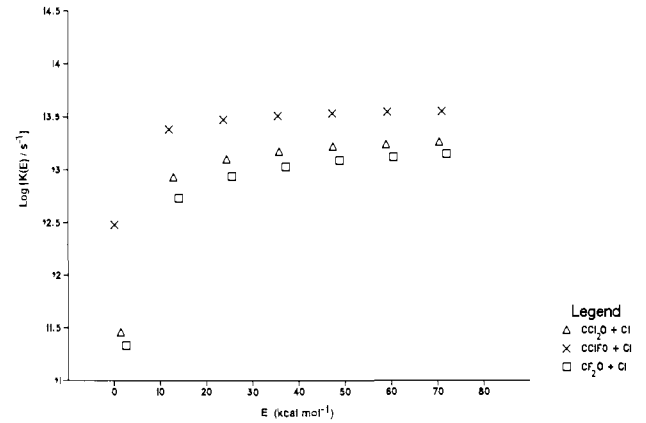

Figure 4. Energy-dependent RRKM rate constants for chlorine atom elimination from CCl_3O, CCl_2FO, and $CClF_2O$ radicals.

The critical energy E_0 for halogen atom eliminations from $CCl_{3-x}F_xO$ was taken to be the best estimate of the dissociation barrier (PMP4SDQ/6-31G* + ΔZPE/3-21G). The moments of inertia for both reactants and transition states were obtained from the UHF/6-31G* optimized geometries (see Table I) and the unscaled UHF/3-21G vibrational frequencies (see Tables II–IV) were employed. Plots of the resulting RRKM rate constants against total energy E are shown in Figures 3 and 4. With the total energy below 100 kcal mol^{-1}, the dissociation rate constants are larger for the Cl atom extrusion processes than for the F atom extrusion processes. A $CCl_{3-x}F_xO$ radical with about 1.0 kcal mol^{-1} of energy in excess of E_0 has a chemical lifetime of less than 10^{-11} s. As shown in Figure 3, greater chlorine substitution on the radical can increase the rate for fluorine elimination, as a consequence of lowering the barrier for the extrusion. Furthermore, the substitution of one chlorine atom by a fluorine atom in CCl_3O, as shown in Figure 4, increases the rate constants of the chlorine atom elimination reaction, but the substitution of two chlorine atoms by two fluorine atoms has the opposite effect, slowing the rate of release of chlorine atom. In this case the reduced density of available states for dissociation which results from higher frequencies modes in the transition state for CCl_2FO contributes to the slower dissociation rate in addition to the increased barrier height. The implications are that on the carbon fragment there should be at least two fluorine atoms to complement the chlorine atom; this would act to retard the release of the chlorine atom. Consequently, $CClF_2O$ may be sufficiently long lived enough to undergo bimolecular reaction. However, we do note that if the $CCl_{3-x}F_3O$ radicals are produced by highly exothermic processes, unimolecular decomposition would dominate. Additionally, comparison of calculated unimolecular rates for CF and CCl bond fission processes (Figures 3 and 4) clearly indicates that the relative rates of chlorine are greater than fluorine eliminations, Cl > F.

Concluding Remarks

The dissociation dynamics of the $CCl_{3-x}F_xO$ (x = 0, 1, 2) radicals have been studied by using ab initio method with spin annihilation. F atom extrusion from Cl-containing species of $CCl_{3-x}F_xO$ radicals is unlikely. The chlorine atom elimination processes are predicted to be low activation energy processes, and at low pressure, these processes will dominate over bimolecular reactions of $CCl_{3-x}F_xO$ with other molecules. The replacement of Cl by F affects the stability of $CCl_{3-x}F_xO$ species. These calculations suggest that the release of chlorine atom from the $CCl_{3-x}F_xO$ could be retarded by the addition of two fluorines to the carbon fragment.

Acknowledgment. We are grateful to Wayne State Universtiy Computer Center and Chemistry Department for provision of computing resources and to the National Science Foundation for a Presidential Young Investigator Award.